IEEE Access
Multidisciplinary | Rapid Review | Open Access Journal

Received May 17, 2019, accepted June 30, 2019, date of publication July 24, 2019, date of current version August 16, 2019.

Digital Object Identifier 10.1109/ACCESS.2019.2930818

Lossless CFA Image Compression Chip Design for Wireless Capsule Endoscopy

CHIUNG-AN CHEN[1], SHIH-LUN CHEN[2], (Member, IEEE), CHI-HAO LIOA[2], AND PATRICIA ANGELA R. ABU[3]

[1]Department of Electrical Engineering, Ming Chi University of Technology, New Taipei 243, Taiwan
[2]Department of Electronic Engineering, Chung Yuan Christian University, Taoyuan 320, Taiwan
[3]Department of Information Systems and Computer Science, Ateneo de Manila University, Quezon 1108, Philippines

Corresponding author: Shih-Lun Chen (chrischen@cycu.edu.tw)

This work was supported in part by the Ministry of Science and Technology (MOST), Taiwan, under Grant MOST-107-2218-E-131-002, Grant MOST-107-2221-E-033-057, Grant MOST-107-2622-E-033-002-CC2, Grant MOST-107-2622-E-131-007-CC3, Grant MOST-106-2622-E-033-014-CC2, Grant MOST-106-2221-E-033-072, and Grant MOST-106-2119-M-033-001, and in part by the National Chip Implementation Center, Taiwan.

ABSTRACT This paper presents a hardware-oriented lossless color filter array (CFA) image compression algorithm for very-large-scale integration (VLSI) circuit design. In order to achieve high performance, low complexity and low memory requirement, a novel lossless CFA image compression algorithm based on JPEG-LS is proposed for the VLSI implementation. A previous study showed the usage of a context table with its memory consuming more than 81% of the chip area for a JPEG-LS encoder design. The proposed algorithm implements a JPEG-LS-based lossless image compression algorithm that eliminates the use of the context technique and its memory in order to reduce the chip area while still maintaining its high performance. The proposed algorithm includes a pixel restoration, an adaptive Golomb–Rice parameter prediction and an improved Golomb–Rice coding technique. This paper was realized using a 0.18μ m CMOS process with synthesized gate counts and core area of 4.8 k and 57,625μm^2, respectively. The synthesized operating frequency of this design reached 200 MHz by using a pipeline scheduling technique. Compared with the previous JPEG-LS-based designs, this paper reduced the gate count to at least 28% and increased the average compression ratio by over 17.15% using the video endoscopy images from the Gastro Gastroenterologist Hospital.

INDEX TERMS Color filter array, context-free, Golomb-Rice, JPEG-LS, lossless compression, VLSI, and wireless capsule endoscopy.

I. INTRODUCTION

Recently, wireless capsule endoscopy provides an innovative methodology to diagnose diseases of digestive systems through a comfortable and efficient manner of examination. Since the capsule endoscopy is swallowed into the human body, the size and frequency of wireless signal transmission is strictly limited. Moreover, since the capsule endoscopy records the status of the digestive system through continues image capture, it consumes a lot of energy to transmit the captured images through wireless transmission. Given the limitations in terms size and energy in wireless transmission, there is a need to develop a low complexity, low memory requirement and low power consumption technique for wireless capsule endoscopy. Given this, a lossless image compression technique is useful in reducing the power and storage space used in wireless capsule endoscopy.

Recently, most of CCD and CMOS image sensors captured photos using color-filter-array (CFA) formats, in which each pixel includes only one color each for Red (R), Green (G) or Blue (B) color. It is more efficient to compress images in CFA format rather than in RGB format since the amount of data in images in CFA format is only one third compared to RGB format. There are many different structures of CFA [1], such as Bayer CFA [2], Lukac and Plataniotis CFA [3], Yamanaka CFA [4], diagonal stripe CFA [3], vertical stripe CFA [3], modified Baer CFA [3] and HVS-based CFA [5]. Since the Bayer CFA [2] is the most popular and widely used in CMOS image sensors, the Bayer CFA format will be used to develop the proposed lossless CFA image compression algorithm.

The associate editor coordinating the review of this manuscript and approving it for publication was Gian Domenico Licciardo.

There are many literatures that inspected the compression algorithms of softwares [6]–[10]. There are also a few novel researches [11]–[19] which provide some efficient methods to compress image data in VLSI architectures. A new approach for near-lossless and lossless image compression algorithm with Bayer color-filter-array was proposed in [6]. JPEG-LS is a standard for lossless and near-lossless compression for continuous-tone images. The processes of the lossless compression of JPEG-LS are as follows: modeling the images in one dimension, calculating the prediction residual values and encoding the prediction residual values.

To implement low-complexity compression algorithm for images, the JPEG-LS image compression standard was proposed in [8]. Many high performance image compression chip designs had been developed for the wireless capsule endoscopy. The JPEG-LS [8] is a popular lossless and near-lossless image compression standard due to its low complexity and high performance. A fast and context-free lossless image compression algorithm based on JPEG-LS was proposed in [9]. A hardware-orient JPEG-LS design was proposed in [11]. It is a low-memory-requirement JPEG-LS VLSI design with a Golomb coding and a run Golomb coding technique with eight-stage pipelined architecture based on LOCO-I algorithm and JPEG-LS VLSI architecture. But a context model is 81% of the total area in the JPEG-LS encoder design. A low-power control design contained a power management unit, a wireless wake-up subsystem and a JPEG-LS encoder was presented in [12]. A memory-free lossless image compressor design based on a combination of Golomb-Rice and unary coding was proposed in [13]. A low-complexity and lossless image compression system based on YEF color space and a variable length predictive scheme was presented in [14].

A fast, efficient, lossless image compression system (FELICS) VLSI-oriented algorithm and its implementation was proposed in [15]. In order to improve the performance of lossless image compression for CFA images, a hybrid entropy coding and color replacement techniques were proposed in [16]. A raw Bayer CFA pattern was proposed for advanced procedure with filtering function of the application of wireless image sensor node and data compressing in [17]. Furthermore, an JPEG-LS encoder [18] was implemented with the component of an efficient pipelined specifically. For the purpose of high performance encoder, a fully pipelined architecture [19] provided with thirteen stages and variable-length for more efficient manner. A color filter array (CFA) is one of the key encoder of lossless compression algorithm. Moreover, a hierarchical predictor and context-adaptive arithmetic for Bayer CFA image that is more efficient was presented in [20]. The process is directing the edges in considered nearby pixels and gathering characteristic with edge activity and neighboring errors. In [21], a low complexity lossless image compression was implemented by an adaptive JPEG-LS. Consequently, the achievement of super high data throughput has updated the context parameters by breaking the feedback loop. In addition, [22] proposed a cost-efficient near-lossless CFA image compressor by using context-free algorithm. It is novel that a pixel restoration, prediction, run mode and entropy encoder were included. In advance, a pipeline technique was provided for performance and gate counts improvement.

According to the discussion in [1]–[22], it is necessary to develop a lossless CFA image compressor design with the characteristics of a low cost, low memory requirement, and high compression ratio for wireless capsule endoscopies. In this paper, a novel ten-stage and pipelined VLSI architecture with low-complexity and high compression ratio lossless image compression VLSI design is proposed. It removes the context modeling to reduce the complexity and cost. By restoring the R, G, B in the Bayer Color-Filter-Array, creating a novel prediction and advanced entropy coding, the compression ratios of the proposed algorithm were improved efficiently.

In this paper, the lossless image compression algorithm is presented in Section II. Section III discusses the proposed pipelined VLSI architecture in this study. Section IV presents the simulation results and chip implementation. Finally, conclusion is presented in Section V.

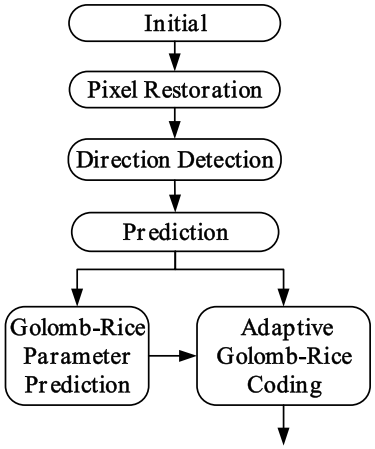

FIGURE 1. Flowchart of the proposed lossless CFA image compression algorithm.

II. LOSSLESS IMAGE COMPRESSION ALGORITHM

Traditionally, JPEG-LS algorithm contains five parts: a context model, a prediction model, a regular mode model, a run mode model and an entropy coding model. To reduce the complexity and memory requirement, it is necessary to remove the context model from the JPEG-LS lossless image compression algorithm. Moreover, since the run mode model is a near-lossless kind of technique this causes a little distortion in the images. Hence, the run mode is not included in the proposed lossless image compression algorithm. As shown in Fig. 1, the proposed lossless compression algorithm only contains a pixel restoration model, a prediction model, a regular mode model, and an entropy coding model with a hybrid technique. At first, the pixel restoration model restores the input data in CFA format to RGB format, and then it tries to find the direction of pixel continuity. Predictor module will

choose the most appropriate predicted value and then transmit it to the encoder. After that, a novel encoder will produce an efficient code.

A. PIXEL RESTORATION

The correlation between neighboring pixels in CFA image is very low. Hence, some efficient arrangements of Bayer CFA image had been used in previous studies [16], [22]. This study proposes a novel arrangement of having the staggered R, G, B that complements a CFA image to turn into three collected classifications as shown in Fig. 2. This offers an efficient way to enhance the correlation of the neighboring pixels to improve the prediction. Furthermore, this proposed arrangement considers and improves on the complexity and memory requirement. The proposed algorithm does not change the arrangement of the color components. As the result, in the proposed novel way, it is unnecessary to apply an additional memory for arranging the CFA images therefore enhancing the compression ratio.

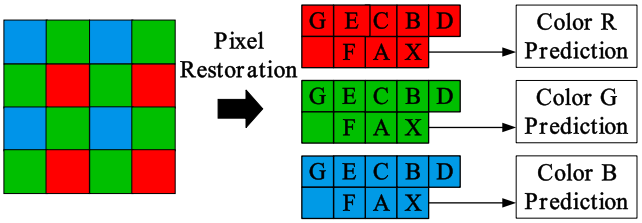

FIGURE 2. Pixel restoration from CFA format to RGB format.

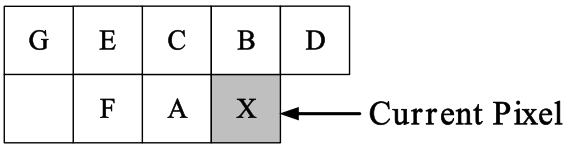

FIGURE 3. The prediction pixel and reference pixels.

B. PREDICTION

Unlike traditional JPEG-LS, gradients and run mode are not used in the proposed algorithm. The prediction pixel values are interpolated from seven neighboring pixels (A-G) according to the prediction directions illustrated in Fig. 3. Because the difference among neighboring pixels directly corresponds to the edge, the proposed algorithm predicts with four possible modes according to the different directions. The proposed method offers four prediction modes: horizontal, vertical, diagonal-down-left and diagonal-down-right as shown in Fig. 4.

We can directly compute all the differences between two neighboring pixels, which corresponds to four major texture directions types namely Type 1: horizontal (h), Type 2: vertical (v), Type 3: diagonal-down-right (ddr), and Type 4: diagonal-down-left (ddl). The four major pixel direction distance strengths can be expressed as shown below

$$D_h = |P_{(x-2,y)} - P_{(x-1,y)}| + |P_{(x-2,y-1)} - P_{(x-1,y-1)}| \quad (1)$$

$$D_v = |P_{(x-2,y-1)} - P_{(x-2,y)}| + |P_{(x-1,y-1)} - P_{(x-1,y)}| \quad (2)$$

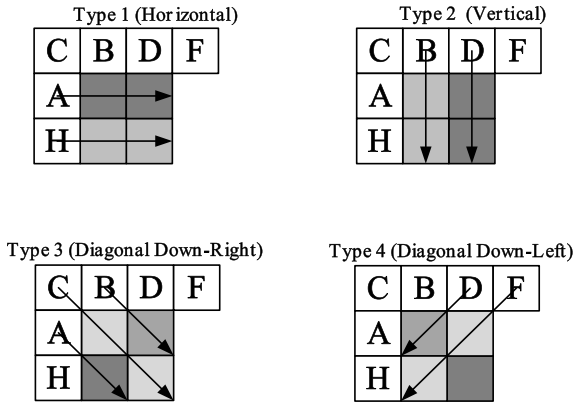

FIGURE 4. Four types of pixel directions.

$$D_{ddr} = |P_{(x-3,y-1)} - P_{(x-2,y)}| + |P_{(x-2,y-1)} - P_{(x-1,y)}| \quad (3)$$

$$D_{ddl} = |P_{(x,y-1)} - P_{(x-1,y)}| + |P_{(x-2,y-1)} - P_{(x-1,y-1)}| \quad (4)$$

where x and y are locations of $P_{(x,y)}$ in the horizontal and vertical directions, respectively.

After computing four types of error strengths in pixel directions, we can assume that the pixel direction is the type which computed the lowest D. After that, the X_{med} is the pixel value prediction by the reference A, B, C, D, E, F, and G. The four types of X_{med} are listed below:

Type 1 (h) : $X_{med} = A$
Type 2 (v) : $X_{med} = B$
Type 3 (ddr): $X_{med} = C$
Type 4 (ddl): $X_{med} = D$

Furthermore, we calculate the residual value-N using Eq. (5) to process entropy coding.

$$N = X_{med} - X \quad (5)$$

The predictor selects the most appropriate X_{med} to calculate with X to send the residual value to next stage.

C. ENTROPY CODING

1) IMPROVED GOLOMB-RICE ENTROPY CODES

After the prediction process, the value of residual value-N can be obtained as a positive or a negative number. In order to encode the positive and negative numbers more efficiently, a novel Golombe-Rice coding was developed and is proposed in this study. This is to decrease the length of the Golomb-Rice code by adding a sign bit to the Golomb-Rice coding as shown in Fig. 5.

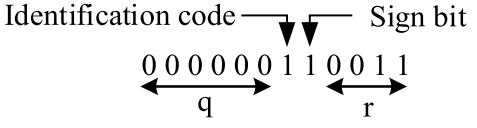

FIGURE 5. Improved Golomb-Rice coding with a sign bit.

As mentioned before, Golomb-Rice coding uses a parameter M to divide N into two parts: q and r. The q is the quotient of N divided into M while k represents the bit number of r.

In this study, the encoder of Golomb-Rice coding with a sign bit can be divided to 4 steps and are as follows:

- Step 1: Add q bits 0s.
- Step 2: Add a bit symbol 1.
- Step 3: Add a bit sign bit symbol 1.
- Step 4: Add k bits binary code of r.

In the original Golomb-Rice coding, it is necessary to use two different codes for two values which have the same absolute number and of different sign. For example, the codes in the original Golomb-Rice coding of $+1$ and -1 are "110" and "101", respectively. Hence, it is necessary to prepare two codes in the codebook for these two different values. However, by using the proposed improved Golomb-Rice Entropy coding, there is only one bit difference between two values which have the same absolute number and of different sign. For example, the codes for the proposed improved Golomb-Rice Entropy coding of $+1$ and -1 when $M = 4$ are "1001" and "1101", respectively. When encoding $+1$ and -1, the codebook only needs to prepare a code "1" encoding q and a code "01" encoding k because q and k are the same in $+1$ and -1. It can reduce the codebook to half as compared to the original Golomb-Rice coding. This therefore efficiently saves hardware cost. Table 1 lists four examples of the improved Golomb-Rice coding with different parameters M.

TABLE 1. Improved Golomb-Rice entropy codes.

N	M	Codes
0	M=2	100
	M=4	1000
	M=8	10000
	M=16	100000
1	M=2	101
	M=4	1001
	M=8	10001
	M=16	100001
-5	M=2	00111
	M=4	01101
	M=8	11101
	M=16	110101
17	M=2	00000000101
	M=4	00001001
	M=8	001001
	M=16	010001

2) EXTEND CODING

The length of code is not increased rapidly when the value of N is increased. Since the Golomb-Rice code is a variable length code (VLC), each quotient value demands a unique code. The length of the Golomb-Rice code will increase rapidly when the value of N increase. The length of Golomb-Rice code will be larger than 8-bit in original pixel value. Therefore, a novel Golombe-Rice coding is proposed in this study to decrease the length of the Golomb-Rice code by adding a sign bit to the Golomb-Rice code. For example, the parameter $M = 4$ and $N = 0$ are represented as 1000 (q is 0, sign is positive and r is 0). In this case, the negative zero code 1100 is useless. Thus, the negative zero codes were used to represent as extend code, which can reduce more bits than the Modified Golomb-Rice code proposed in [22]. Some examples are illustrated as follows:

1) 110 when $M = 2$
2) 1100 when $M = 4$
3) 11000 when $M = 8$, and
4) 110000 when $M = 16$

As shown in Table 1, the length of the extend code and extend value is much less than that of the original Golomb-Rice coding. Hence, the proposed novel Golomb-Rice coding technique can efficiently improve the compression ratios.

This study encodes the N by the improved Golomb-Rice entropy coding usually. When N is too large to encode by the novel Golomb-Rice entropy coding, it will be encoded by the extend coding. Besides, in the proposed novel Golomb-Rice entropy coding, every number N contains four type of codes as shown in Table 2. The encode region of the proposed novel Golomb-Rice entropy coding can be changed by M as below.

TABLE 2. Entropy codes of this work.

N	M	Codes
1	M=2	101
	M=4	1001
	M=8	10001
	M=16	100001
-1	M=2	111
	M=4	1101
	M=8	11001
	M=16	110001
63	M=2	11001001111
	M=4	110001001111
	M=8	000000010111
	M=16	000101111
-87	M=2	11001010001
	M=4	110001010001
	M=8	1100001010001
	M=16	00000110001

When $M = 2$, the proposed novel Golomb-Rice entropy coding encode region is -17 to $+17$, extend coding region is -255 to -17 and 17 to 255, as shown in Fig. 6(a).

When $M = 4$, the proposed novel Golomb-Rice entropy coding encode region is -35 to $+35$, extend coding region is -255 to -35 and 35 to 255, as shown in Fig. 6(b).

When $M = 8$, the proposed novel Golomb-Rice entropy coding encode region is -71 to $+71$, extend coding region is -255 to -35 and 35 to 255, as shown in Fig. 6(c).

When $M = 16$, the proposed novel Golomb-Rice entropy coding encode region is -143 to $+143$, extend coding region is- 255 to -143 and 143 to 255, as shown in Fig. 6(d).

If the N is divided by a larger parameter $M = 16$, the code length is shorter. Hence, this study presents a novel methodology by using an adjustable parameter M for each N called adaptive Golomb-Rice parameter prediction which will be described next section.

To conclude these two sections, this work tries to use a shorter code to encode the high probability N. If the code length after encoding is much longer than the original bit

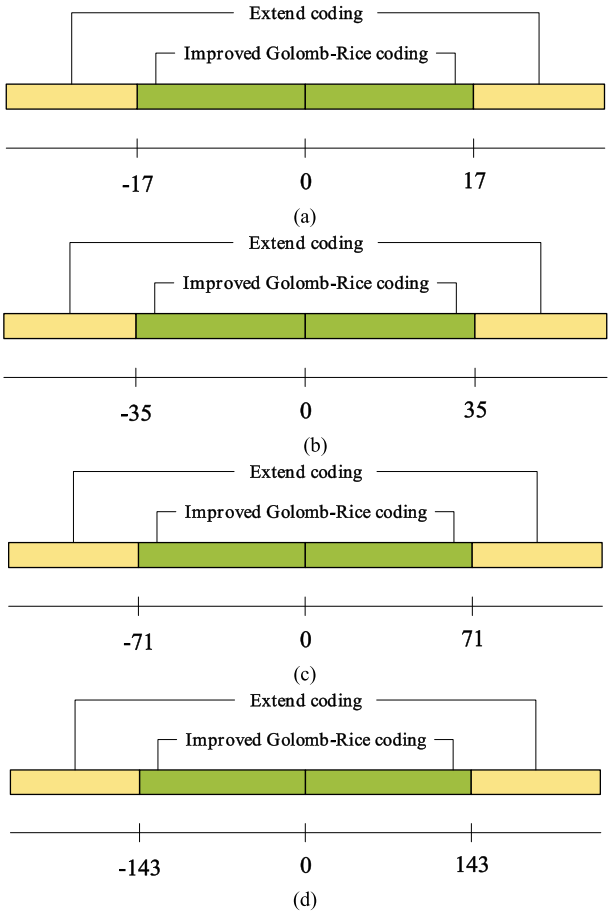

FIGURE 6. Encode regions of (a) $M = 2$, (b) $M = 4$, (c) $M = 8$ and (d) $M = 16$.

number, extend coding will be used. Table 2 shows the entropy codes of this work.

D. ADAPTIVE GOLOMB-RICE PARAMETER PREDICTION

Golomb-Rice is a classic entropy coding technique that is suitable for hardware implementation due to its low complexity. For example, if the value of N is large and it is divided by parameter $M = 2$, the code length of quotient q will be longer. In contrast, if the N is divided by a larger parameter $M = 16$, the code length would be shorter. Hence, this study presented a novel methodology by using an adjustable parameter M for each N, called adaptive Golomb-Rice parameter prediction. By this technique, the parameter M can be predicted according to the information of the previous values of M.

By using the proposed novel methodology, when using Golomb-Rice coding to encode the first predicted value N, the parameter M for encoding the first predicted value N is fixed to $M = 2$. The code length of quotient q can be obtained using N and M. Since the prediction trends in neighboring pixels are close, we use the quotient q of the current pixel to predict the value of parameter M for the next pixel. For example, if the value of quotient q in the first pixel is 4 when the first parameter M is fixed to 2, we will use 4 as the predicted parameter M to encode the next predicted value. Hence, it is unnecessary to include and compress any value of M to the bit-stream. Each value of M can be predicted by the value of q with the processed previously predicted value N. The q and r for encoding next N are obtained by using the predicted parameter M to divide the next N. Since the values of N in the same color have high correlation, the proposed adaptive Golomb-Rice parameter prediction method can improve the compression ratio efficiently.

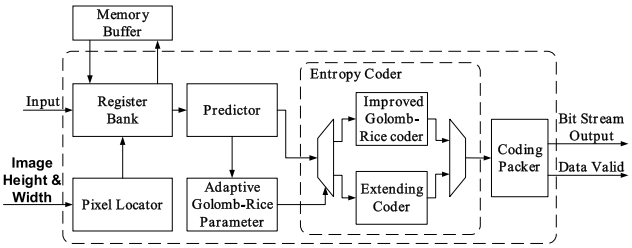

FIGURE 7. Block diagram of proposed lossless compression encoder.

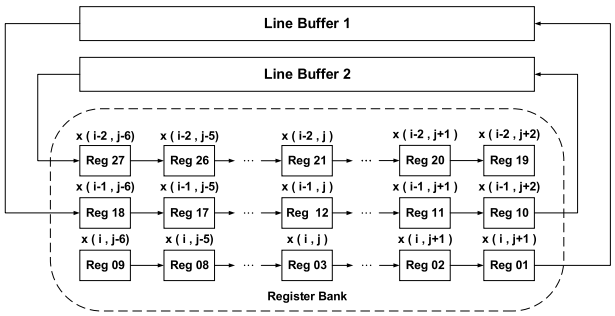

FIGURE 8. Architecture of the register bank.

III. VLSI ARCHITECTURE

Fig. 7 shows the architecture of the proposed lossless CFA image encoder. It is composed of a register bank, a predictor module, a pixel locator, an adaptive Golomb-Rice parameter, an improved Golomb-Rice coder, an extending coder and a coding packer. The register bank is connected to a memory buffer, as shown in Fig. 8, to provide four neighboring pixels sequentially *Ra*, *Rb*, *Rc*, and *Rd* for prediction. In addition, in order to improve the performance remarkably, the proposed design was implemented using a nine-stage pipeline architecture as shown in Fig. 14. The details of the pixel locator and the four main modules are illustrated as follows.

A. PIXEL LOCATOR

Since the colors of the reference pixels *A, B, C, D, E, F* and *G* are all not the same as the color of the prediction candidate pixel *X* as shown in Fig. 2, a pixel locator is needed to find the correct reference pixels in memory. A register bank was designed with a two-line-buffer memory, as shown in Fig. 8, to provide the pixel values for the prediction module. First, the image sensor captures Bayer CFA raw data and then fills into the register bank sequentially. Next, the register bank

pushes the data into the line buffer. At the end of the *line buffer1*, the data are filled into the second row of register for the pixel locator and predictor. The register bank is used to provide the positions *A, B, C, D, E, F, G* and *X* of the Bayer CFA pixels. Furthermore, a boundary detector is added to the proposed design and is used to find the boundary information in order to avoid wrong colors when the boundary regions are located by a boundary detector.

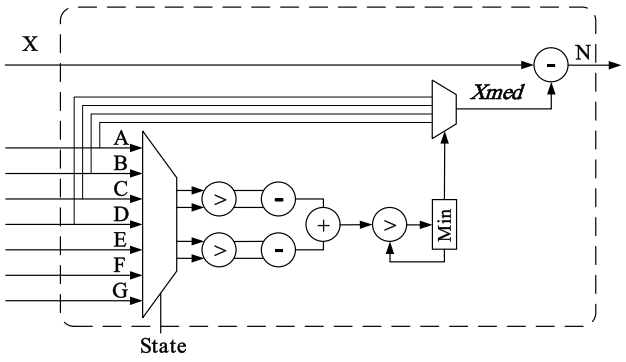

FIGURE 9. Architecture of direction error strengths calculator.

B. PREDICTOR

In order to reduce the cost of the hardware in this study, a hardware sharing and finite state machine (FSM) are used. Since the proposed direction error strengths calculator was designed through hardware sharing, it needs four cycles to generate a result. Fig. 9 shows the architecture of the proposed direction error strengths calculator, where the input pixels *A, B, C, D, E, F* and *G* are selected according to the FSM signal *State* in order to compare the direction error strengths with the different direction types. After computing four types of direction error strengths, the predicted result X_{med} is produced.

C. ENTROPY CODER

The code of the encoder is composed of *q* bits "0", a symbol bit "1", a sign bit "1" and a *P* bit as *r*. The code length is the sum of *q*, 2 (a symbol bit "1", a sign bit "1") and *M*.

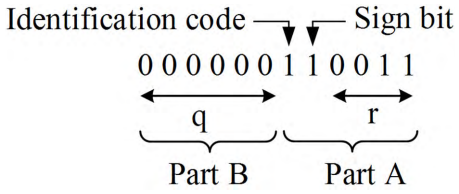

FIGURE 10. Composition of code.

Furthermore, the code is divided into two parts as shown in Fig. 10. Part A is the code combination following the identification code as shown in Fig. 10. Part B is the code before the identification code which are all 0 codes from *q* is defined by the code length of the packer module. The packer module will be discussed in detail in the next section.

As presented above, the improved Golomb-Rice entropy code is composed of *r*-bits 0, a bit of identification code, a bit of sign bit and *M* bit of *r*. Consequently, the code length of each encoded pixel is different from others. The longest code is 15 bits whereas the shortest code is 3 bits only. In hardware design, a register cannot change its size arbitrarily, thus the register via the transmitting code size must be set up to 15 bits. When the bits of the encoded code are shorter than 15 bits, the high-order bits will be padded with 0s. The code register will transmit a wrong code to the next stage. In this system, the signal code length is applied to fix this problem which is the wrong code propagating. The operation generates a code length through a shifter and an adder. The code of extending is a simple combination that consists of an extended code and the residual value *N* as shown in Fig. 11. At first, the multiplexer selects 4 inputs over *P* to generate the extended code.

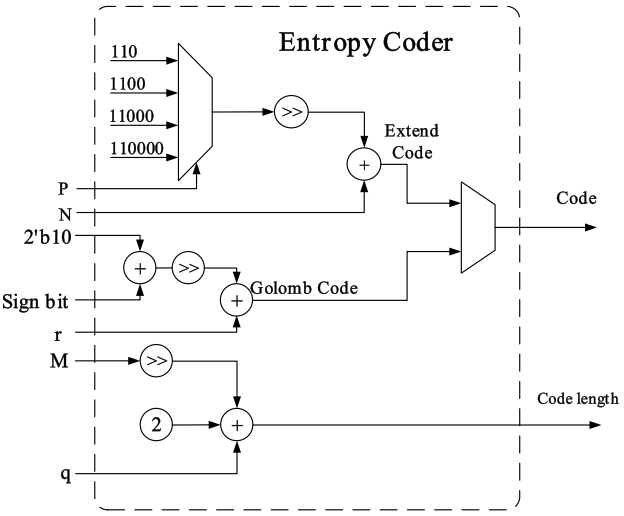

FIGURE 11. Architecture of the entropy coder.

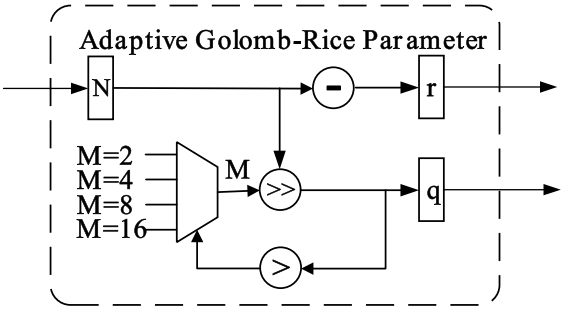

FIGURE 12. Architecture of adaptive Golomb-Rice parameter module.

D. ADAPTIVE GOLOMB-RICE PARAMETER MODULE

This module consists of a multiplexer, a comparator, a subtractor, a shifter, and three registers as shown in Fig. 12. The generator of a parameter is produced shifter values of *q* and *r* in order to instead of a divider, which purposed reduction of the hardware cost efficiently. The value of *q* is stored in

a register and is sent to a comparator right after. Following with comparing the value of q and intervals, a selection signal is produced to select one of the four M parameters through the use of a multiplexer. The selected M parameter is used to divide the value of the next N. Hence, the performance of Golomb-Rice Coding is improved because a suitable parameter M will be selected for the next N by the proposed design of the adaptive Golomb-Rice parameter module.

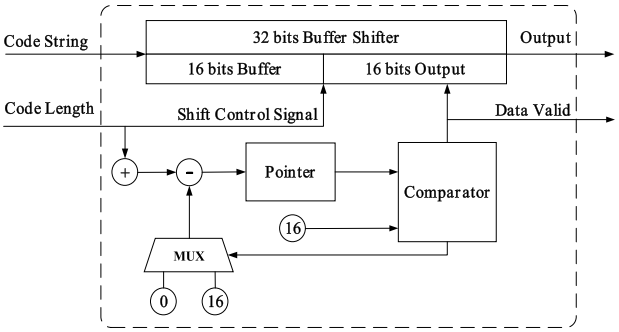

FIGURE 13. Architecture of the coding packer.

E. CODING PACKER

The coding packer is an influential part in the entropy coding affectivity. On the basis of each code, from residual N has a different length. The packer restores the codes for the specific 16-bit utmost and sends a valid output in 16-bit data as shown in Fig. 13. The width of the register used for storing the codes is 15 bits. Therefore, if the register code is transmitted directly to the coding packer module, the packer will generate a wrong code. The length and codes are sent to the coding packer concurrently. The coding packer will shift the 32-bit buffer-shifter several times depending on the code length of the encoded codes. After shifting, adding the register code to the 32-bit buffer-shifter is required. Consequently, the coding packer will receive the correct codes.

F. PIPELINE ARCHITECTURE

The proposed lossless compression encoder was designed as a nine-stage pipelined architecture to improve performance. The following are the details for each stage.

Stage 1: The pixel locator determines the positions of A, B, C, D, E, F, G and X which are from the Bayer CFA by counting the height and width of the image while encoding at the beginning. Further, the prediction pixel and the reference pixels are transmitted from the register bank to the prediction module for the propose of residual value predicting. The pixel locator sends an enable signal to the prediction module meanwhile encoder module.

Stage 2 - Stage 5: At the begin, the predictor computes the error strengths of the directions and chooses the mode in the lowest cost in order to achieve the predicted pixel. Afterwards, it sends the positive value of the prediction residual and a bit sign signal to the next stage.

Stage 6: The adaptive Golomb-Rice parameter module produces the values of q and r, and the predicted parameter M. The parameter module adjusts M according to the variety of q.

Stage 7: The entropy coding selector determines which combination of entropy coding to apply, then sends the signal of controlling to the next stage.

Stage 8: The coding modules receive the residual value, sign and controlling signals of prediction, and generate the codes and lengths of strings to the next stage.

Stage 9: The coding packer receives the size code uncertainty. The most important task is to sort out the problem of 16-bit codes and send the codes and valid signal immediately.

By these techniques and concepts, the benefits of the operating complexity, gate counts, and chip area are greatly reduced. Moreover, the performance of this VLSI architecture have minimized the gate count.

IV. SIMULATION RESULTS AND CHIP IMPLEMENTATION

In this study, we used Matlab to verify the feasibility of the proposed lossless CFA image compression algorithm. First, we used the system level design simulation results to make the goal of the complexity and compression ratios. After determining the algorithm, Verilog codes were written according to the developed algorithm. Next, the Verilog codes were processed by logic synthesis with a Design Compiler tool to transfer the design to gate level codes and then simulate the gate level codes using Verdi tool. Then, an IC Compiler tool is utilized to produce the layout graph to tape out the chip at the Chip Implement Center (CIC), Taiwan. Finally, this chip was fabricated by TSMC company. The chips were tested and were measured using an FPGA board, logic analysis and ADVANTEST V93000 PS1600 Automatic Test System.

Eight testing images from [23] with the size of 352 $\times$ 240 pixels captured by the video endoscopy by [22] were selected as the testing dataset and are shown in Fig. 15. These original color testing images is in full RGB format with 352 $\times$ 240 R, G and B pixels in each endoscopy image.

Table 3 and Table 4 show the simulation results of the compression ratios and bit per pixel for JPEG-LS [11], CFA-LS [16] and this work for the eight endoscopy images from the Hereditary Telangiectasia2 dataset [22]. The results show that the average compression ratios of this work were improved to 39.4% and 17.15% than the previous studies JPEG-LS [11] and CFA-LS [16], respectively. The average bit per pixel is 4.4677 in this work which is much less than 5.4448 and 6.4788 in previous studies JPEG-LS [11] and CFA-LS [16], respectively. Because JPEG-LS [11], CFA-LS [16] and this work are all lossless image compression techniques, it is unnecessary to compare the refined image quality.

Table 5 and Table 6 list the bit per pixels results of seven endoscopy videos from Hereditary Telangiectasia1 Hereditary Telangiectasia1 [22] dataset with 9,767 total

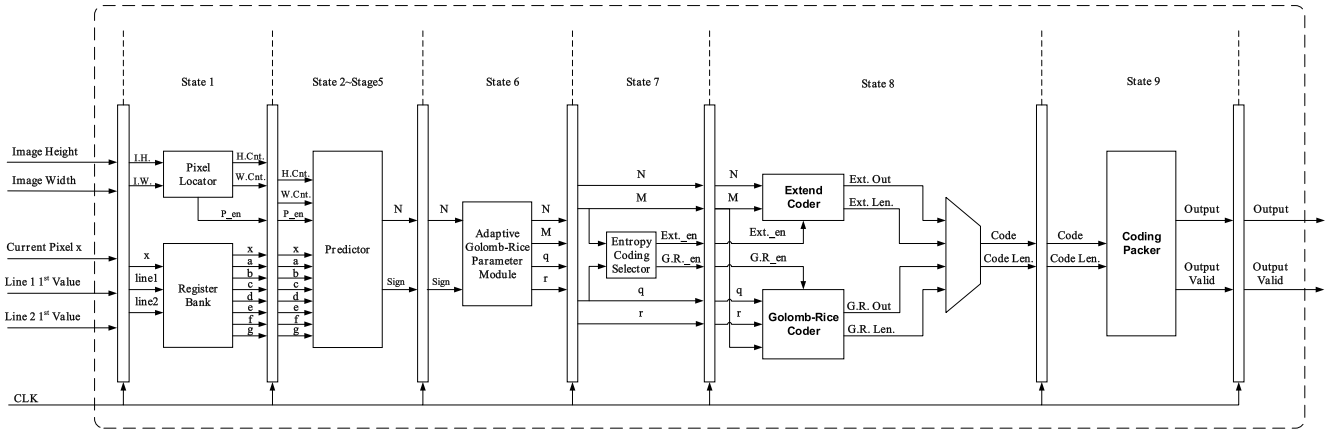

FIGURE 14. Nine-Stage pipelined architecture of the proposed lossless compression encoder circuit.

TABLE 3. Comparison of lossless compression ratios for eight endoscopic images.

	JPEG-LS [11]	CFA-LS [16]	This Work
Image format	Bayer CFA	Bayer CFA	Bayer CFA
(a)	1.3547	1.5889	1.8407
(b)	1.2073	1.4428	1.6952
(c)	1.1673	1.4008	1.6538
(d)	1.0561	1.2915	1.5425
(e)	1.1319	1.3657	1.6173
(f)	1.2854	1.5180	1.7704
(g)	1.2157	1.4527	1.7032
(h)	1.4606	1.6943	1.9477
Average	**1.2348**	**1.4693**	**1.7213**

TABLE 4. Comparison of bit per pixel values for eight endoscopic images.

	JPEG-LS [11]	CFA-LS [16]	This Work
Image format	Bayer CFA	Bayer CFA	Bayer CFA
(a)	5.0349	5.9054	4.3462
(b)	5.5448	6.6264	4.7192
(c)	5.7110	6.8534	4.8373
(d)	6.1943	7.5750	5.1864
(e)	5.8578	7.0678	4.9465
(f)	5.2701	6.2237	4.5188
(g)	5.5070	6.5806	4.6970
(h)	4.7217	5.4772	4.1074
Average	**5.4448**	**6.4788**	**4.6477**

TABLE 5. Comparison of lossless compression ratios for seven endoscopy videos.

	JPEG-LS [11]	CFA-LS [16]	This Work
Image format	Bayer CFA	Bayer CFA	Bayer CFA
H_T1 (985frames)	1.1563	1.5726	1.7055
H_T2(1942frames)	1.2171	1.4939	1.7145
H_T3(1212frames)	1.2350	1.4351	1.7417
H_T4(1425frames)	1.2003	1.4127	1.6939
H_T5(1065frames)	1.2827	1.4071	1.5640
H_T6(1686frames)	1.3146	1.4857	1.6414
H_T7(1452frames)	1.2577	1.4730	1.6739
Average	**1.2376**	**1.4685**	**1.6764**

amount of frames. The average compression ratio for 9,767 frames achieved by this work is 1.6249, which is 39.6% better than 1.2326 for JPEG-LS [11] and 14% better than

TABLE 6. Comparison of bit per pixel values for seven endoscopy videos.

	JPEG-LS [11]	CFA-LS [16]	This Work
Image format	Bayer CFA	Bayer CFA	Bayer CFA
H_T1 (985frames)	6.9186	5.0871	4.6907
H_T2(1942frames)	6.5730	5.3551	4.6661
H_T3(1212frames)	6.4777	5.5745	4.5932
H_T4(1425frames)	6.6650	5.6629	4.7228
H_T5(1065frames)	6.2368	5.6855	5.1151
H_T6(1686frames)	6.0855	5.3847	4.8739
H_T7(1452frames)	6.3608	5.4311	4.7793
Average	**6.4641**	**5.4477**	**4.9234**

TABLE 7. Comparison of lossless compression ratios for four classic color images.

	JPEG-LS [11]	CFA-LS [16]	This Work
Image format	Bayer CFA	Bayer CFA	Bayer CFA
(a)	1.5364	1.5309	1.6242
(b)	1.2792	1.4028	1.5014
(c)	1.0744	1.4551	1.5031
(d)	1.0402	1.4703	1.5028
Average	**1.2326**	**1.4648**	**1.5323**

TABLE 8. Comparison of bit per pixel values for four classic color images.

	JPEG-LS [11]	CFA-LS [16]	This Work
Image format	Bayer CFA	Bayer CFA	Bayer CFA
(a)	5.2069	5.2257	4.9255
(b)	6.2539	5.7029	5.3284
(c)	7.4460	5.4979	5.3223
(d)	7.6908	5.4411	5.3233
Average	**6.4903**	**5.4615**	**5.2248**

1.4648 for CFA-LS [16]. To compare the results, we can easily find that the proposed algorithm is more suitable for capsule endoscopy images and videos.

Table 7 and Table 8 list the compression ratios and bit per pixel results of JPEG-LS [11], CFA-LS [16] and the proposed algorithm using the four classic testing images namely Airplane, House, Lena and Peppers. The four popular 512×512 selected as the testing dataset and are shown in Fig. 16. In this study, we used Matlab tool to verify the feasibility of the proposed lossless algorithm compared with the

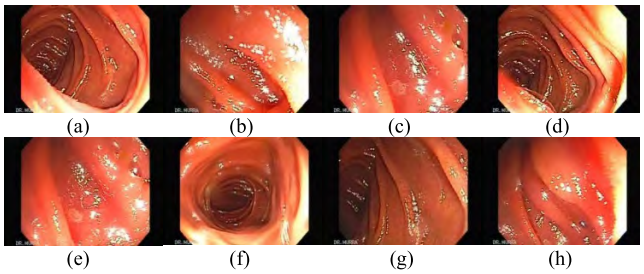

FIGURE 15. Testing endoscopy images dataset from Gastro Gastroenterologist Hospital [23] (a) Image of Hereditary_Telangiectasia2 1497 (b) Image of Hereditary_Telangiectasia2 0221. (c) Image of Hereditary_Telangiectasia2 0300 (d) Image of Hereditary_Telangiectasia2 0071 (e) Image of Hereditary_Telangiectasia2 0298. (f) Image of Hereditary_Telangiectasia2 06. (g) Image of Hereditary_Telangiectasia2 0043 (h) Image of Hereditary_Telangiectasia3 1933.

TABLE 9. Comparison with previous lossless compression algorithms.

	JPEG-LS [11]	[16]	This Work
Image format	Bayer CFA	Bayer CFA	Bayer CFA
1	1.2360	1.2093	1.2688
2	1.1345	1.5555	1.6211
3	1.3670	1.6438	1.7619
4	1.2158	1.4898	1.5706
5	1.2282	1.1584	1.2610
6	1.3105	1.3259	1.4285
7	1.3786	1.5252	1.6220
8	1.2855	1.1908	1.1988
9	1.5738	1.5615	1.6383
10	1.4793	1.5420	1.6039
11	1.3669	1.4039	1.4748
12	1.4212	1.5790	1.6588
13	1.1709	1.0671	1.1927
14	1.2348	1.2773	1.3658
15	1.3731	1.5777	1.6420
16	1.4242	1.4805	1.5806
17	1.6134	1.4976	1.5672
18	1.2955	1.2668	1.3605
19	1.4590	1.3869	1.4598
20	1.7903	1.6647	1.7403
21	1.3373	1.3688	1.4954
22	1.2326	1.4040	1.4577
23	1.2155	1.6623	1.7745
24	1.4034	1.3305	1.3813
Avg.	**1.3411**	**1.4237**	**1.5053**

JPEG-LS standard compression algorithm [11] and a lossless CFA compression algorithm [16]. The average compression ratios of the proposed lossless compression algorithm are

FIGURE 16. Four testing images (a) Airplane (b) House (c) Lena (d) Peppers.

1.5323 and 5.2248 in bit per pixel. These are much better than 1.2326 and 6.4903 in bit per pixel of the JPEG-LS standard [11] by over 24%.

In order to objectively test the algorithm, the Kodak dataset that includes 24 images with a size of 768 × 512 pixels was selected as testing patterns. Fig. 17 shows the 24 images of Kodak dataset. The average compression ratio of the proposed algorithm is 1.5053, which is 12.24% better than 1.3411 for JPEG-LS [11] and 5.73% better than 1.4237 for CFA-LS [16].

The proposed lossless CFA image compression algorithm was implemented by using a hardware description language (HDL) Verilog and synthesized by using an electronic design automation (EDA) tool Design Vision. This work was synthesized using 0.18μm CMOS process. It contained 4.8 K NAND-equivalent gate counts and is operated at 200 MHz frequency with a core area of 57,625 μm^2. Compared with previous designs presented in [11]–[13], [15], [16], [18], [22], the proposed design was able to reduce more than 28% gate counts and required least memory except for [13].

Fig. 18 shows the micrograph of the proposed fabricated chip, with a chip dimension of 240μm x 240μm. The chip was tested using the ADVANTEST V93000 PS1600 Automatic Test System. Fig. 19 shows the measurement

TABLE 10. Comparison with previous lossless compression encoder designs by synthesis results.

	[18]	[11]	[12]	[15]	[13]	[14]	[16]	[22]	This work
Year	2007	2009	2009	2010	2013	2014	2015	2016	2018
Process (μm)	0.18	FPGA	0.18	0.18	0.18	FPGA	0.18	0.18	0.18
Frequency (MHz)	183	21	20	200	42	N/A	200	80	200
Power (mW)	N/A	N/A	1.3	4.1	1.78	1.63	2.2	3.1	4.5
Gate Counts (K)	27.6	37.3	19.5	11.6	24	N/A	5.54	12.4	4.8
Memory (kbits)	20.8	146	17.5	15.2	0	0	10.2	10.2	10.2
Normalized Area	6.39	8.63	4.51	2.68	5	N/A	1.28	2.58	1

Note: The normalized area is normalized by NAND-equivalent gate counts

FIGURE 17. Twenty-four testing images of Kodak dataset.

TABLE 11. Specifics of the proposed lossless CFA image compression chip design.

	This Work
Gate Count	4.8 K NAND Gates
Frequency	120 MHz
Power Consumption	5.2 mW
Chip Area	240μm×240μm

environment and Fig. 20 is the Shmoo image which represents the highest frequency of this chip design work with undistorted. The measurement results of the proposed lossless CFA image compression chip design are listed in Table 11.

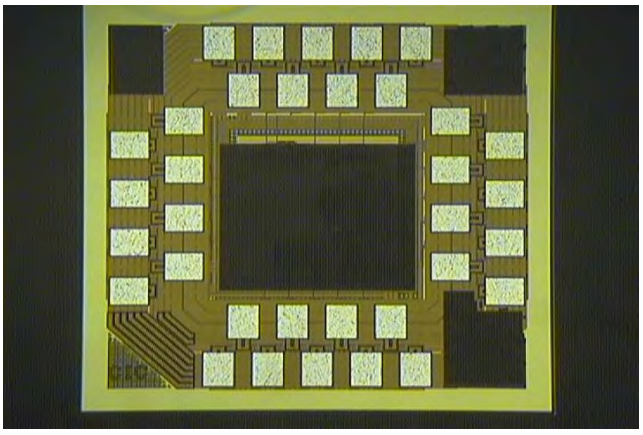

FIGURE 18. Micrograph of the proposed adaptive local backlight control chip fabricated by using TSMC 0.18-μm CMOS process.

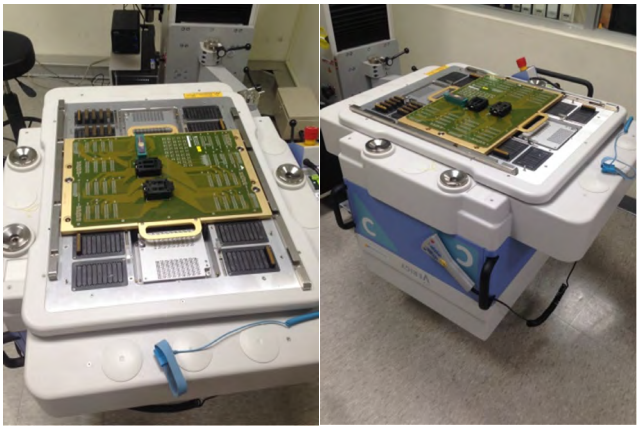

FIGURE 19. Measurement environment with ADVANTEST V93000 PS1600 automatic test system.

FIGURE 20. Shmoo image of this proposed.

V. CONCLUSION

In this paper, a novel hardware-oriented lossless CFA image compression algorithm that is based on a pixel restoration, an adaptive Golomb-Rice parameter prediction and an improved Golomb-Rice coding techniques is proposed. This chip design have the benefits of higher compression ratio and lower hardware cost than previously proposed lossless image compression designs that makes the proposed design suitable for the development of wireless capsule endoscopy.

REFERENCES

[1] W.-J. Yang, K.-L. Chung, W.-N. Yang, and L.-C. Lin, "Universal chroma subsampling strategy for compressing mosaic video sequences with arbitrary RGB color filter arrays in H.264/AVC," *IEEE Trans. Circuits Syst. Video Technol.*, vol. 23, no. 4, pp. 591–606, Apr. 2013.

[2] B. E. Bayer, "Color imaging array," U.S. Patent 3 971 065 A, Jul. 20, 1976.
[3] R. Lukac and K. N. Plataniotis, "Color filter arrays: Design and performance analysis," *IEEE Trans. Consum. Electron.*, vol. 51, no. 4, pp. 1260–1267, Nov. 2005.
[4] S. Yamanaka, "Solid state color camera," U.S. Patent 4 054 906 A, Oct. 18, 1977.
[5] M. Parmar and S. J. Reeves, "A perceptually based design methodology for color filter arrays [image reconstruction]," in *Proc. IEEE Int. Conf. Acoust., Speech, Signal Process.*, May 2004, p. 473.
[6] X. Xie, G. Li, X. Li, Z. Wang, C. Zhang, D. Li, and L. Zhang, "A new approach for near-lossless and lossless image compression with Bayer color filter arrays," in *Proc. 3rd Int. Conf. Image Graph.*, Dec. 2004, pp. 357–360.
[7] M. J. Weinberger, J. Rissanen, and R. B. Arps, "Applications of universal context modeling to lossless compression of gray-scale images," *IEEE Trans. Image Process.*, vol. 5, no. 4, pp. 575–586, Apr. 1996.
[8] M. J. Weinberger, G. Seroussi, and G. Sapiro, "The LOCO-I lossless image compression algorithm: Principles and standardization into JPEG-LS," *IEEE Trans. Image Process.*, vol. 9, no. 8, pp. 1309–1324, Aug. 2000.
[9] Y. Gera, Z. Wang, S. Simon, and T. Richter, "Fast and context-free lossless image compression algorithm based on JPEG-LS," in *Proc. Data Compress. Conf.*, Snowbird, UT, USA, Apr. 2012, p. 396.
[10] P. G. Howard and J. S. Vitter, "Fast and efficient lossless image compression," in *Proc. Data Compress. Conf.*, Snowbird, UT, USA, Mar./Apr. 1993, pp. 351–360.
[11] P. Merlino and A. Abramo, "A fully pipelined architecture for the LOCO-I compression algorithm," *IEEE Trans. Very Large Scale Integr. (VLSI) Syst.*, vol. 17, no. 7, pp. 967–971, Jul. 2009.
[12] X. Chen, X. Zhang, L. Zhang, X. Li, N. Qi, H. Jiang, and Z. Wang, "A wireless capsule endoscope system with low-power controlling and processing ASIC," *IEEE Trans. Biomed. Circuits Syst.*, vol. 3, no. 1, pp. 11–22, Feb. 2009.
[13] T. H. Khan and K. A. Wahid, "Lossless and low-power image compressor for wireless capsule endoscopy," *VLSI Des.*, vol. 2011, no. 3, Jan. 2011, Art. no. 343787. doi: 10.1155/2011/343787.
[14] T. H. Khan and K. A. Wahid, "Design of a lossless image compression system for video capsule endoscopy and its performance in *in-vivo* trials," *Sensors*, vol. 14, no. 11, pp. 20779–20799, 2014.
[15] T. H. Tsai, Y. H. Lee, and Y. Y. Lee, "Design and analysis of high-throughput lossless image compression engine using VLSI-oriented FELICS algorithm," *IEEE Trans. Very Large Scale Integr. (VLSI) Syst.*, vol. 18, no. 1, pp. 39–52, Jan. 2010.
[16] S. L. Chen, Y. R. Chen, T. L. Lin, and Z. Y. Liu, "A cost-efficient lossless compression color filter array images VLSI design for wireless capsule endoscopy," *J. Med. Imag. Health Inform.*, vol. 5, no. 3, pp. 378–384, May 2015.
[17] X. Chen, H. Jiang, X. W. Li, and Z. Wang, "A novel compression method for wireless image sensor node," in *Proc. IEEE Asian Solid-State Circuits Conf.*, Jeju, South Korea, Nov. 2007, pp. 184–187.
[18] M. Papadonikolakis, V. Pantazis, and A. P. Kakarountas, "Efficient high-performance ASIC implementation of JPEG-LS encoder," in *Proc. Design, Automat. Test Eur. Conf. Exhib.*, Apr. 2007, pp. 1–6.
[19] B.-S. Kim, S. Baek, D.-S. Kim, and D.-J. Chung, "A high performance fully pipeline JPEG-LS encoder for lossless compression," *IEICE Electron. Express*, vol. 10, no. 12, Jun. 2013, Art. no. 20130348.
[20] S. Kim and N. I. Cho, "Lossless compression of color filter array images by hierarchical prediction and context modeling," *IEEE Trans. Circuits Syst. Video Technol.*, vol. 24, no. 6, pp. 1040–1046, Jun. 2014.
[21] Z. Wang, T. Zhang, L. Yan, and C. Gong, "A high performance fully pipelined architecture for lossless compression of satellite image," in *Proc. Int. Conf. Multimedia Technol.*, Oct. 2010, pp. 1–4.
[22] S.-L. Chen, T.-Y. Liu, C.-W. Shen, and M.-C. Tuan, "VLSI implementation of a cost-efficient near-lossless CFA image compressor for wireless capsule endoscopy," *IEEE Access*, vol. 4, pp. 10235–10245, 2016.
[23] Gastroenterologist Hospital. *El Salvador Atlas of Gastrointestinal Video Endoscopy*. [Online]. Available: http://www.gastrointestinalatlas.com

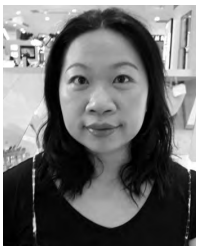

CHIUNG-AN CHEN received the B.S. degree in electronic engineering from Chung Yuan Christian University, Zhongli, Taoyuan, Taiwan, in 2005, and the Ph.D. degree in electrical engineering from National Cheng Kung University, Tainan, Taiwan, in 2013. Since 2017, she has been an Assistant Professor with the Department of Electrical Engineering, Ming Chi University of Technology, Taiwan. Her current research interests include VLSI chip design, image processing, wireless body sensor networks, the Internet of Things, wearable devices, and bio-medical signal and image processing.

SHIH-LUN CHEN (M'12) received the B.S., M.S., and Ph.D. degrees from National Cheng Kung University, Tainan, Taiwan, in 2002, 2004, and 2011, respectively, all in electrical engineering. He was an Assistant Professor with the Department of Electronic Engineering, Chung Yuan Christian University in Taiwan, from 2011 to 2014, and an Associate Professor with the Department of Electronic Engineering, Chung Yuan Christian University, Taiwan, from 2014 to 2017, where he has been a Professor with the Department of Electronic Engineering, since 2017. His current research interests include VLSI chip design, image processing, wireless body sensor networks, the Internet of Things, wearable devices, data compression, fuzzy logic control, bio-medical signal processing, and reconfigureable architecture.

Dr. Chen was a recipient of the Outstanding Teaching Award from Chung Yuan Christian University, in 2014.

CHI-HAO LIOA received the B.S. and M.S. degrees from the Department of Electronic Engineering, Chung Yuan Christian University, Zhongli, Taoyuan, Taiwan, in June 2015 and 2017, respectively. His current research interests include VLSI chip design and image processing.

PATRICIA ANGELA R. ABU received the B.S. degree in electronics and communications engineering from the Ateneo de Manila University, Philippines, in 2007, the M.S. degree in electronic engineering (majoring in microelectronics) from Chung Yuan Christian University, Zhongli, Taoyuan, Taiwan, in 2009, and the Ph.D. degree in computer science from the Ateneo de Manila University, in 2015, where she has been an Assistant Professor with the Department of Information Systems and Computer Science, since 2015.